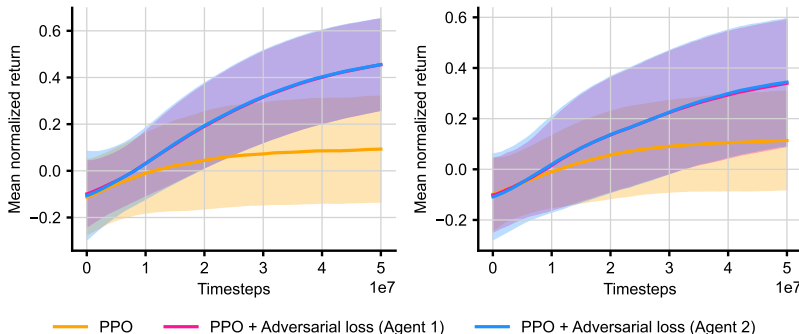


# A DUAL-AGENT ADVERSARIAL FRAMEWORK FOR GENERALIZABLE REINFORCEMENT LEARNING

000  
001  
002  
003  
004  
005 **Anonymous authors**  
006 Paper under double-blind review  
007  
008  
009  
010

## ABSTRACT

011 Recently, empowered with the powerful capabilities of neural networks, reinforcement  
012 learning (RL) has successfully tackled numerous challenging tasks. How-  
013 ever, while these models demonstrate enhanced decision-making abilities, they  
014 are increasingly prone to overfitting. For instance, a trained RL model often  
015 fails to generalize to even minor variations of the same task, such as a change in  
016 background color or other minor semantic differences. To address this issue, we  
017 propose a dual-agent adversarial policy learning framework, which allows agents  
018 to spontaneously learn the underlying semantics without introducing any human  
019 prior knowledge. Specifically, our framework involves a game process between  
020 two agents: each agent seeks to maximize the impact of perturbing on the op-  
021 ponent’s policy by producing representation differences for the same state, while  
022 maintaining its own stability against such perturbations. This interaction encour-  
023 ages agents to learn generalizable policies, capable of handling irrelevant fea-  
024 tures from the high-dimensional observations. Extensive experimental results on  
025 the Procgen benchmark demonstrate that the adversarial process significantly im-  
026 proves the generalization performance of both agents, while also being applied to  
027 various RL algorithms, e.g., Proximal Policy Optimization (PPO). With the adver-  
028 sarial framework, the RL agent outperforms the baseline methods by a significant  
029 margin, especially in hard-level tasks, marking a significant step forward in the  
030 generalization capabilities of deep reinforcement learning.



031  
032  
033  
034  
035  
036  
037  
038  
039  
040  
041  
042  
043 **Figure 1: Comparisons of the generalization capability of different RL agents.** By applying our  
044 adversarial approach to PPO, the two adversarial PPO agents demonstrate significant improvements  
045 in train performance (left) and test performance (right) across eight environments in the *hard-level*  
046 Procgen benchmark. In this context, higher scores indicate better generalization capabilities.  
047

## 1 INTRODUCTION

050 Reinforcement Learning (RL) has emerged as a powerful paradigm for solving complex decision-  
051 making problems, leveraging an agent’s ability to learn from interactions with an environment  
052 through trial and error (Sutton, 2018). However, generalization between tasks remains difficult for  
053 state-of-the-art deep reinforcement learning algorithms. Although trained agents can solve complex  
tasks, they often struggle to transfer their experience to new environments. For instance, an agent

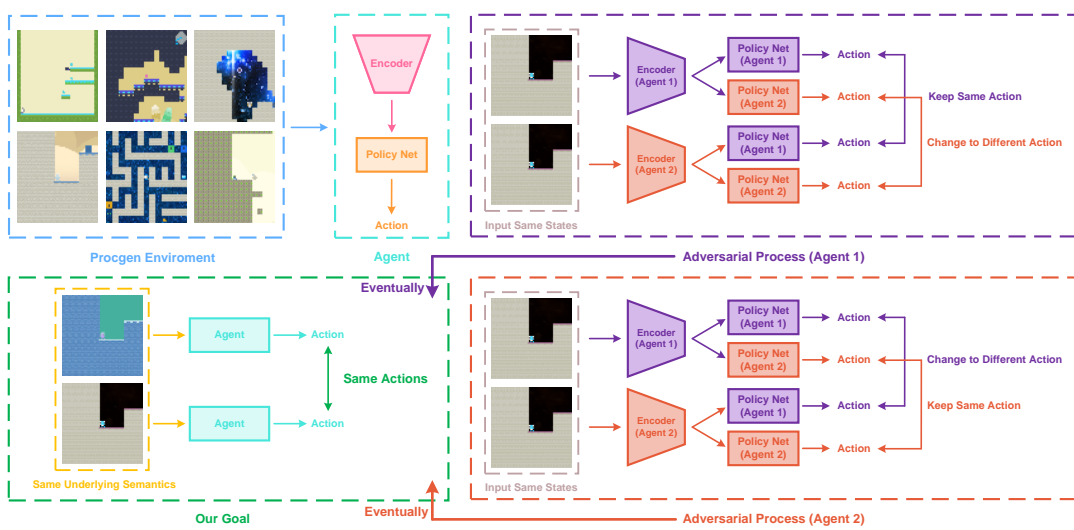


Figure 2: **Overview of the adversarial process.** Our method involves a game process between two homogeneous agents, as shown in the figure. The training samples are simultaneously input into the encoders of both agents, resulting in differing representations for the same observation. By adjusting the parameters of the two encoders, both agents aim to ensure that their own policy networks are robust to such differences while maximizing the influence of these differences on the other agent’s policy network as much as possible. This minimax game process will eventually allow robust policy learning, preventing agents from overfitting to irrelevant features in high-dimensional observations, thereby enhancing generalization performance.

trained in a specific environment struggles to perform effectively in another, even when the only difference between environments is a subtle alteration, such as the change of colors in the scene (Cobbe et al., 2019; 2020). This limitation underscores the challenges of transferring knowledge across different contexts, emphasizing the importance of developing robust generalization strategies for RL applications in dynamic and variable real-world scenarios (Korkmaz, 2024).

One approach to enhancing generalization in RL focuses on data augmentation techniques (Lee et al., 2019; Laskin et al., 2020; Zhang & Guo, 2021), which increase the diversity of training data by modifying input observations or environmental conditions. While this provides a straightforward solution, it can introduce biases that do not align with RL objectives and often neglect the nuances of the RL process, potentially limiting effectiveness. Another approach involves regularizing the learned functions, drawing from traditional techniques used in deep neural networks, such as batch normalization (Liu et al., 2019), contrastive learning (Agarwal et al., 2021), and loss function regularization (Amit et al., 2020). However, these methods can not adequately address the unique challenges of RL, as they often focus on static representations rather than the dynamic nature of agent-environment interactions. Consequently, both data augmentation and traditional regularization methods have limitations that hinder their ability to facilitate effective generalization in RL.

Adversarial learning (Pinto et al., 2017; Zhang et al., 2020; Oikarinen et al., 2021; Li et al., 2021; Rahman & Xue, 2023) presents a promising direction for enhancing generalization in RL by learning robust representations of irrelevant features through an adversarial process. This framework facilitates the development of agents capable of adapting to new environments by emphasizing the distinction between relevant and irrelevant information. While adversarial learning frameworks integrate the RL process, existing methods often rely on introducing generator and discriminator networks (Goodfellow et al., 2014) or seek to modify fundamental parameters of the simulation environments. Such heterogeneous adversarial processes introduce additional hyperparameters and training costs, necessitating carefully designed architectures. These complexities make it challenging to establish a unified framework for generalization tasks across diverse domains.

To address the generalization problem in RL, in this paper, we propose a novel adversarial learning framework, which involves a game process between two homogeneous agents (in Figure 2). This framework offers three key advantages: 1). First, this general framework can integrate well

with existing policy learning algorithms such as Proximal Policy Optimization (PPO) (Schulman et al., 2017). 2). Second, the adversarial process allows agents to spontaneously learn the underlying semantics without necessitating additional human prior knowledge, thus fostering robust generalization performance. 3). Lastly, our approach introduces minimal additional hyperparameters, highlighting its potential for widespread applicability across various RL models. Extensive experiments demonstrate that our adversarial framework significantly improves generalization performance in Procgen (Cobbe et al., 2020), particularly in hard-level environments (in Figure 1). This framework marks a significant advancement in addressing generalization challenges in deep reinforcement learning.

Our contributions are summarized as follows:

- To the best of our knowledge, we are the first to theoretically prove that minimizing the policy’s robustness to irrelevant features helps improve generalization performance.
- We propose a general adversarial learning framework to improve the generalization performance of agents, which is compatible with existing policy learning algorithms.
- Extensive results demonstrate that applying the adversarial framework to standard RL baselines gains significant improvements in generalization performance.

## 2 PRELIMINARIES

**Markov Decision Process and Generalization Settings.** We first consider the formalization of generalization in RL. Denote a Markov Decision Process (MDP) as  $m$ , defined by the tuple

$$m = (\mathcal{S}_m, \mathcal{A}, r_m, \mathcal{P}_m, \rho_m, \gamma), \quad (1)$$

where  $m$  is sampled from the distribution  $p_{\mathcal{M}}(\cdot)$ ,  $\mathcal{S}_m$  represents the state space,  $\mathcal{A}$  represents the action space,  $r_m : \mathcal{S}_m \times \mathcal{A} \mapsto \mathbb{R}$  is the reward function,  $\mathcal{P}_m : \mathcal{S}_m \times \mathcal{A} \times \mathcal{S}_m \mapsto [0, 1]$  is the probability distribution of the state transition function,  $\rho_m : \mathcal{S}_m \mapsto [0, 1]$  is the probability distribution of the initial state, and  $\gamma \in (0, 1]$  is the discount factor. Typically, during training, the agent is only allowed to access  $\mathcal{M}_{\text{train}} \subset \mathcal{M}$  and is then tested for its generalization performance by extending to the entire distribution  $\mathcal{M}$ . The agent generates the following trajectory on  $m$ :

$$\tau_m = (s_0^m, a_0^m, r_0^m, \dots, s_t^m, a_t^m, r_t^m, \dots). \quad (2)$$

Similar to standard RL, the state-value function, value function can be defined as

$$Q_m^\pi(s_t^m, a_t^m) = \mathbb{E}_{s_{t+1}^m, a_{t+1}^m, \dots} \left[ \sum_{k=0}^{\infty} \gamma^k r_m(s_{t+k}^m, a_{t+k}^m) \right], \quad V_m^\pi(s_t^m) = \mathbb{E}_{a_t^m \sim \pi(\cdot | s_t^m)} [Q_m^\pi(s_t^m, a_t^m)]. \quad (3)$$

Given  $Q_m^\pi$  and  $V_m^\pi$ , the advantage function can be expressed as  $A_m^\pi(s_t^m, a_t^m) = Q_m^\pi(s_t^m, a_t^m) - V_m^\pi(s_t^m)$ . We now denote  $\zeta(\pi) = \mathbb{E}_{m \sim p_{\mathcal{M}}(\cdot), \tau_m \sim \pi} [\sum_{t=0}^{\infty} \gamma^t r_m(s_t^m, a_t^m)]$  as the generalization objective given policy  $\pi$ , and denote  $\eta(\pi) = \mathbb{E}_{m \sim p_{\mathcal{M}_{\text{train}}}(\cdot), \tau_m \sim \pi} [\sum_{t=0}^{\infty} \gamma^t r_m(s_t^m, a_t^m)]$  as the training objective, where the notation  $\mathbb{E}_{\tau_m \sim \pi}$  indicates the expected return of the trajectory  $\tau_m$  generated by the agent following policy  $\pi$ , i.e.,  $s_0^m \sim \rho_m(\cdot)$ ,  $a_t^m \sim \pi(\cdot | s_t^m)$ ,  $r_t^m \sim r_m(s_t^m, a_t^m)$ ,  $s_{t+1}^m \sim \mathcal{P}_m(\cdot | s_t^m, a_t^m)$ , where  $t \in \mathbb{N}$ ,  $\mathbb{N}$  is the set of all natural numbers.

For the convenience of subsequent theoretical analysis, we decouple the state  $s_t^m$  into  $u_t$  and  $\phi_m(\cdot)$ , i.e.,  $s_t^m = \phi_m(u_t)$ , where  $u_t$  is independent of  $m$ , while  $\phi_m(\cdot)$  is completely and only determined by  $m$ . For instance,  $u_t$  implicitly encompasses significant semantic information, which is crucial for the agent to maximize the expected return. This includes, for example, the relative positional relationship between the manipulated character and obstacles in its surroundings. On the other hand, the function  $\phi_m$  obfuscates these pieces of information, such as the background or rendering style of the game. This suggests that even two vastly different states may represent identical semantics, making it seemingly implausible for an agent utilizing a Convolutional Neural Network (CNN) for feature extraction to maintain robustness against such variations.

Therefore, the generalization of reinforcement learning has been proven to be highly challenging (Ghosh et al., 2021), as the agent may use the additional information provided by  $\phi_m$  to “cheat”. In some extreme cases, the agent can achieve high scores solely by memorizing these additional pieces

of information, while lacking any comprehension of the underlying semantics, which can further lead to the agent completely failing on unseen  $m \sim p_{\mathcal{M}}(\cdot)$ .

Hence, we attempt to eliminate the influence of  $m$ . We consider a Hidden Markov Decision Process (HMDP) that consists entirely of useful information (in other words, all variables that can be affected by  $m$  are excluded from consideration), denote it as  $m^* = (\mathcal{U}, \mathcal{A}, r, \mathcal{P}, \rho, \gamma)$ .

### 3 THEORETICAL ANALYSIS

In this section, we derive the lower bounds for the training and generalization performance of the agent. The main conclusion drawn from this is that improving the agent's robustness to irrelevant features will help enhance its generalization performance.

Given the probability distribution  $p_{\mathcal{M}}$ , we first make the following assumption:

**Assumption 3.1.** When  $m$  is sampled from  $\mathcal{M}_{\text{train}} \subset \mathcal{M}$ , i.e.,  $m \sim p_{\mathcal{M}_{\text{train}}}(\cdot)$ , we assume that

$$p_{\mathcal{M}_{\text{train}}}(m) = \frac{p_{\mathcal{M}}(m) \cdot \mathbb{I}(m \in \mathcal{M}_{\text{train}})}{M}, \quad (4)$$

where  $M = \int_{\mathcal{M}_{\text{train}}} p_{\mathcal{M}}(m) dm$  is the normalized coefficient that represents the probability that  $m$ , sampled from the entire distribution  $\mathcal{M}$ , belongs to  $\mathcal{M}_{\text{train}}$ , while  $\mathbb{I}(\cdot)$  is the indicator function.

It can be proved that  $p_{\mathcal{M}_{\text{train}}}(m)$  is a probability distribution, please refer to Appendix C.1 for details. Based on Assumption 3.1, we can derive the following generalization theorem:

**Theorem 3.2** (Generalization performance lower bound). *Given any policy  $\pi$ , the following bound holds:*

$$\zeta(\pi) \geq \eta(\pi) - \frac{2r_{\max}}{1-\gamma} \cdot (1-M), \quad (5)$$

where  $\zeta(\pi)$  and  $\eta(\pi)$  denote the generalization objective and training objective, respectively;  $r_{\max} = \max_{m,s,a} |r_m(s, a)|$ .

The proof is in Appendix C.2. This inspires us that when sampling  $m$  from the entire  $\mathcal{M}$ , with the increase of  $M$  (i.e., the probability of the sampled  $m \in \mathcal{M}_{\text{train}}$ ), the lower bound of generalization performance is continuously optimized and tends to be consistent with  $\zeta$  when  $M = 1$ .

According to Theorem 3.2, once  $\mathcal{M}_{\text{train}}$  is determined, the value of  $M$  is also fixed, at this point,  $\eta$  is the only term that we can optimize in the lower bound. Therefore, we now focus on optimizing  $\eta$ . Before that, we present some important theoretical results in the following:

**Theorem 3.3.** (Kakade & Langford, 2002) *Let  $\mathbb{P}(s_t = s|\pi)$  represents the probability of the  $t$ -th state equals to  $s$  in trajectories generated by the agent following policy  $\pi$ , and  $\rho_{\pi}(s) = \sum_{t=0}^{\infty} \gamma^t \mathbb{P}(s_t = s|\pi)$  represents the unnormalized discounted visitation frequencies. Given any two policies,  $\pi$  and  $\tilde{\pi}$ , their performance difference can be measured by*

$$\eta(\tilde{\pi}) = \eta(\pi) + \mathbb{E}_{s \sim \rho_{\tilde{\pi}}(\cdot), a \sim \tilde{\pi}(\cdot|s)} [A^{\pi}(s, a)]. \quad (6)$$

**Theorem 3.4.** (Schulman, 2015) *Given any two policies,  $\pi$  and  $\tilde{\pi}$ , the following bound holds:*

$$\eta(\tilde{\pi}) \geq L_{\pi}(\tilde{\pi}) - \frac{4\gamma \max_{s,a} |A^{\pi}(s, a)|}{(1-\gamma)^2} \cdot D_{\text{TV}}^{\max}(\pi, \tilde{\pi})^2, \quad (7)$$

where  $L_{\pi}(\tilde{\pi}) = \eta(\pi) + \mathbb{E}_{s \sim \rho_{\pi}(\cdot), a \sim \tilde{\pi}(\cdot|s)} [A^{\pi}(s, a)]$ .

The aforementioned theorems only consider standard RL. On this foundation, we further extend them and derive a lower bound for the training objective:

**Theorem 3.5** (Training performance lower bound). *Let  $\mathbb{P}(s_t^m = s|m, \pi)$  represents the probability of the  $t$ -th state equals to  $s$  in trajectories generated by the agent following policy  $\pi$  in MDP  $m$ , and  $\rho_{\pi}^m(s) = \sum_{t=0}^{\infty} \gamma^t \mathbb{P}(s_t^m = s|m, \pi)$  represents the unnormalized discounted visitation frequencies. Given any two policies,  $\pi$  and  $\tilde{\pi}$ , the following bound holds:*

$$\eta(\tilde{\pi}) \geq L_{\pi}(\tilde{\pi}) - \frac{4\gamma A_{\max}}{(1-\gamma)^2} \cdot \left( \sqrt{\mathfrak{D}_1} + \sqrt{\mathfrak{D}_2} + \sqrt{\mathfrak{D}_3} \right)^2, \quad (8)$$

---

216 **Algorithm 1** Policy iteration algorithm guaranteeing non-decreasing training performance  $\eta$ 

---

217  
 218 1: **Initialize:** policy  $\pi_0$   
 219 2: **for**  $i = 0, 1, 2, \dots$  **do**  
 220 3:     Solve the constrained optimization problem through

$$\begin{aligned} 221 \quad \pi_{i+1} &\leftarrow \arg \max_{\pi} L_{\pi_i}(\pi) - \eta(\pi_i) - M_{\pi_i}(\pi) \\ 222 \quad \text{s.t.} \quad L_{\pi_i}(\pi) - \eta(\pi_i) &\geq M_{\pi_i}(\pi) \\ 223 \end{aligned}$$


---

224 4: **end for**

---

227 where  $A_{\max} = \max_{m,s,a} |A_m^\pi(s, a)|$ , and

$$\begin{aligned} 229 \quad \eta(\tilde{\pi}) &= \eta(\pi) + \mathbb{E}_{m \sim p_{\mathcal{M}_{\text{train}}}(\cdot), s \sim \rho_{\tilde{\pi}}^m(\cdot), a \sim \tilde{\pi}(\cdot|s)} [A_m^\pi(s, a)], \\ 230 \quad L_\pi(\tilde{\pi}) &= \eta(\pi) + \mathbb{E}_{m \sim p_{\mathcal{M}_{\text{train}}}(\cdot), s \sim \rho_{\pi}^m(\cdot), a \sim \tilde{\pi}(\cdot|s)} [A_m^\pi(s, a)], \\ 231 \quad \mathfrak{D}_1 &= \mathbb{E}_{m \sim p_{\mathcal{M}_{\text{train}}}(\cdot)} \left\{ D_{\text{TV}}^{\max} [\pi(\cdot|\phi_m(u)), \tilde{\pi}(\cdot|\phi_m(u))]^2 \right\}, \\ 232 \quad \mathfrak{D}_2 &= \mathbb{E}_{m, \tilde{m} \sim p_{\mathcal{M}_{\text{train}}}(\cdot)} \left\{ D_{\text{TV}}^{\max} [\pi(\cdot|\phi_m(u)), \pi(\cdot|\phi_{\tilde{m}}(u))]^2 \right\}, \\ 233 \quad \mathfrak{D}_3 &= \mathbb{E}_{m, \tilde{m} \sim p_{\mathcal{M}_{\text{train}}}(\cdot)} \left\{ D_{\text{TV}}^{\max} [\tilde{\pi}(\cdot|\phi_m(u)), \tilde{\pi}(\cdot|\phi_{\tilde{m}}(u))]^2 \right\}, \\ 234 \quad \mathfrak{D}_4 &= \mathbb{E}_{m, \tilde{m} \sim p_{\mathcal{M}_{\text{train}}}(\cdot)} \left\{ D_{\text{TV}}^{\max} [\pi(\cdot|\phi_m(u)), \tilde{\pi}(\cdot|\phi_{\tilde{m}}(u))]^2 \right\}, \\ 235 \quad \mathfrak{D}_5 &= \mathbb{E}_{m, \tilde{m} \sim p_{\mathcal{M}_{\text{train}}}(\cdot)} \left\{ D_{\text{TV}}^{\max} [\tilde{\pi}(\cdot|\phi_m(u)), \tilde{\pi}(\cdot|\phi_{\tilde{m}}(u))]^2 \right\}, \\ 236 \end{aligned} \tag{9}$$

237 where the notation  $D_{\text{TV}}^{\max}(\cdot) = \max_u D_{\text{TV}}(\cdot)$ .

239 The proof see Appendix C.3. This inspires us that  $\mathfrak{D}_1$  measures the difference between the old and  
 240 new policies, while  $\mathfrak{D}_2$  and  $\mathfrak{D}_3$  represent the robustness of the old and new policies to irrelevant  
 241 features of the high-dimensional observations, respectively. Thus

$$243 \quad \eta(\tilde{\pi}) - \eta(\pi) \geq L_\pi(\tilde{\pi}) - \eta(\pi) - C \cdot \left( \sqrt{\mathfrak{D}_1} + \sqrt{\mathfrak{D}_2} + \sqrt{\mathfrak{D}_3} \right)^2, \tag{10}$$

245 where  $C = 4\gamma A_{\max}/(1-\gamma)^2$ . We now denote  $M_\pi(\tilde{\pi}) = C \cdot (\sqrt{\mathfrak{D}_1} + \sqrt{\mathfrak{D}_2} + \sqrt{\mathfrak{D}_3})^2$ , we can then  
 246 derive the following monotonic improvement theorem:

247 **Theorem 3.6** (Monotonic improvement of training performance). *Let  $\pi_0, \pi_1, \pi_2, \dots, \pi_k$  be the se-  
 248 quence of policies generated by Algorithm 1, then*

$$250 \quad \eta(\pi_k) \geq \eta(\pi_{k-1}) \geq \dots \geq \eta(\pi_0). \tag{11}$$

252 *Proof.* According to inequality (10) and Algorithm 1, we have

$$254 \quad \eta(\pi_{i+1}) - \eta(\pi_i) \geq L_{\pi_i}(\pi_{i+1}) - \eta(\pi_i) - M_{\pi_i}(\pi_{i+1}) \geq 0, \tag{12}$$

255 where  $i = 0, 1, \dots, k-1$ , so that  $\eta(\pi_{i+1}) \geq \eta(\pi_i)$ , concluding the proof.  $\square$

257 On the other hand, it is evident that

$$259 \quad \eta(\pi_{i+1}) - \frac{2r_{\max}}{1-\gamma} \cdot (1-M) \geq \eta(\pi_i) - \frac{2r_{\max}}{1-\gamma} \cdot (1-M), \tag{13}$$

262 which means through the iterative process of Algorithm 1, we optimize the lower bound of gen-  
 263 eralization performance (5) as well. In fact, if both  $\mathfrak{D}_2$  and  $\mathfrak{D}_3$  are always equal to zero, i.e., given  
 264 any  $m, \tilde{m} \in \mathcal{M}$  and  $u \in \mathcal{U}$ , we have  $\pi_i(\cdot|\phi_m(u)) = \pi_i(\cdot|\phi_{\tilde{m}}(u))$ ,  $\forall i \in \mathbb{N}$ . In this case, the agent  
 265 has complete insight into the underlying semantics without any influence from  $m$ , thus the agent is  
 266 essentially interacting with  $m^* = (\mathcal{U}, \mathcal{A}, r, \mathcal{P}, \rho, \gamma)$ , Theorem 3.5 degenerates into Theorem 3.4.

267 However, Algorithm 1 is an idealized approach, we have to adopt some heuristic approximations in  
 268 practical solutions. In the following section, we will discuss the specific details of these approxi-  
 269 mations and introduce our proposed dual-agent adversarial framework to overcome the difficulty in  
 optimizing the lower bound (10), which constitutes the core of this paper.

270    **4 METHODOLOGY**  
 271

272    In the previous section, we derived the lower bound of training performance, which inspires us to  
 273    optimize the part of the policy that determines robustness. Therefore, in this section, we first analyze  
 274    the optimization problem of parameterized policies (Section 4.1), then deconstruct what properties  
 275    a generalization agent should have (Section 4.2), and finally propose a dual-agent adversarial frame-  
 276    work to solve the generalization problem (Section 4.3).

277    **4.1 OPTIMIZATION OF PARAMETERIZED POLICIES**  
 278

280    We first consider the parameterized policies, i.e.,  $\pi_\theta$ , and denote the upstream encoder of the pol-  
 281    icy network as  $\psi_w$ , where  $w$  and  $\theta$  represent the parameters of the encoder and policy network,  
 282    respectively.

283    For any given state  $s = \phi_m(u)$ , for brevity, we denote  $\bar{s}_m = \psi_w(\phi_m(u))$  as the representation  
 284    input into the policy network  $\pi_\theta$  after passing through the encoder  $\psi_w$ . Similar to TRPO (Schulman,  
 285    2015), the total variational distance and KL divergence satisfy  $D_{\text{TV}}^{\max} [\pi_{\theta_{\text{old}}}(\cdot|\bar{s}_m), \pi_\theta(\cdot|\bar{s}_m)]^2 \leq$   
 286     $D_{\text{KL}}^{\max} [\pi_{\theta_{\text{old}}}(\cdot|\bar{s}_m), \pi_\theta(\cdot|\bar{s}_m)]$ , where  $\theta_{\text{old}}$  represents the policy network parameters before the up-  
 287    date, while  $\theta$  represents the current policy network parameters. Through heuristic approximation,  
 288    the maximum KL divergence  $D_{\text{KL}}^{\max}$  is approximated as the average KL divergence  $\mathbb{E}[D_{\text{KL}}]$ , and  
 289    then Algorithm 1 is approximated as the following constrained optimization problem:

$$\begin{aligned} \max_{\theta} J(\theta) &= L_{\theta_{\text{old}}}(\theta) - \eta(\theta_{\text{old}}), \\ \text{s.t. } &\begin{cases} \mathbb{E}_{m \sim p_{\mathcal{M}_{\text{train}}}(\cdot)} \{D_{\text{KL}} [\pi_{\theta_{\text{old}}}(\cdot|\bar{s}_m), \pi_\theta(\cdot|\bar{s}_m)]\} \leq \delta_1, \\ \mathbb{E}_{m, \tilde{m} \sim p_{\mathcal{M}_{\text{train}}}(\cdot)} \{D_{\text{KL}} [\pi_\theta(\cdot|\bar{s}_m), \pi_\theta(\cdot|\bar{s}_{\tilde{m}})]\} \leq \delta_2, \end{cases} \end{aligned} \quad (14)$$

295    where  $m$  and  $\tilde{m}$  are MDPs independently sampled from the distribution  $p_{\mathcal{M}_{\text{train}}}$ . Then, similar to  
 296    TRPO,  $J(\theta)$  can be expressed as

$$J(\theta) = \mathbb{E}_{m, s; a \sim \pi_\theta(\cdot|\bar{s}_m)} [A_m^\pi(s, a)] = \mathbb{E}_{m, s; a \sim \pi_{\theta_{\text{old}}}(\cdot|\bar{s}_m)} \left[ \frac{\pi_\theta(a|\bar{s}_m)}{\pi_{\theta_{\text{old}}}(a|\bar{s}_m)} \cdot A_m^\pi(s, a) \right], \quad (15)$$

300    which is called importance sampling, where  $m \sim p_{\mathcal{M}_{\text{train}}}(\cdot)$  and  $s \sim \rho_{\pi_{\theta_{\text{old}}}}^m(\cdot)$ . Thus, we can further  
 301    transform the constrained optimization problem (14) into the following form:

$$\begin{aligned} \max_{\theta} J(\theta) &= \mathbb{E}_{m, s; a \sim \pi_{\theta_{\text{old}}}(\cdot|\bar{s}_m)} \left[ \frac{\pi_\theta(a|\bar{s}_m)}{\pi_{\theta_{\text{old}}}(a|\bar{s}_m)} \cdot \hat{A}(s, a) \right], \\ \text{s.t. } &\begin{cases} \mathbb{E}_{m \sim p_{\mathcal{M}_{\text{train}}}(\cdot)} \{D_{\text{KL}} [\pi_{\theta_{\text{old}}}(\cdot|\bar{s}_m), \pi_\theta(\cdot|\bar{s}_m)]\} \leq \delta_1, \\ \mathbb{E}_{m, \tilde{m} \sim p_{\mathcal{M}_{\text{train}}}(\cdot)} \{D_{\text{KL}} [\pi_\theta(\cdot|\bar{s}_m), \pi_\theta(\cdot|\bar{s}_{\tilde{m}})]\} \leq \delta_2, \end{cases} \end{aligned} \quad (16)$$

308    where  $\hat{A}(s, a)$  is the estimation of the advantage function, and in this paper, we adopt the GAE  
 309    (Schulman et al., 2015) technique. The first constraint of (16) measures the difference between the  
 310    old and new policies, where TRPO (Schulman, 2015) and PPO (Schulman et al., 2017) have already  
 311    provided corresponding solutions. However, it's important to note that the second constraint in (16)  
 312    can not be approximated, as it involves different states with the same underlying semantics, and  
 313    predicting another  $\phi_{\tilde{m}}(u)$  based on any received state  $\phi_m(u)$  ( $m \neq \tilde{m}$ ) is untraceable.

314    Hence, understanding different states with the same underlying semantics is the most central chal-  
 315    lenge in the generalization of deep reinforcement learning. In the following section, we will sys-  
 316    tematically discuss the characteristics a sufficiently general agent should possess to achieve good  
 317    generalization performance.

318    **4.2 HOW TO ACHIEVE GOOD GENERALIZATION?**  
 319

321    As discussed previously, it is unable to solve the optimization problem (16) directly, as the expec-  
 322    tation  $\mathbb{E}_{m, \tilde{m} \sim p_{\mathcal{M}_{\text{train}}}(\cdot)} \{D_{\text{KL}} [\pi_\theta(\cdot|\bar{s}_m), \pi_\theta(\cdot|\bar{s}_{\tilde{m}})]\}$  cannot be estimated due to the unknown distri-  
 323    bution  $p_{\mathcal{M}_{\text{train}}}$  and function  $\phi_m$ . In this section, we focus on analyzing the characteristics that a  
 324    generalization agent should possess.

324

325

326

327

328

329

330

331

332

333

334

335

336

337

338

339

340

341

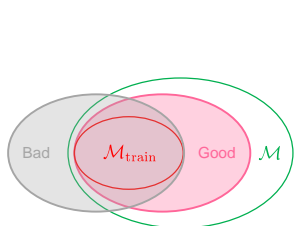
342

343

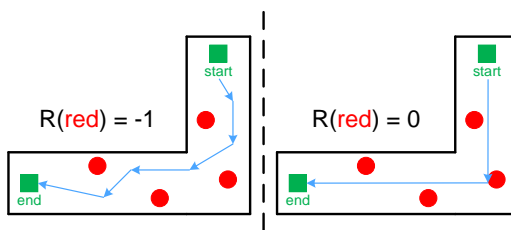
344

345

346



(a) **The impact of biases on generalization.** Among them, the areas enclosed by the red and green curves represent the space of  $M_{\text{train}}$  and  $M$ , respectively, and the area enclosed by the pink curve represents the bias that is beneficial to the generalization of the model, as it is more aligned with  $M$ . The area enclosed by the gray curve represents the bias that may affect the model's generalization, as it is less aligned with  $M$ .



(b) **The impact of reward functions on generalization.** We build a simple maze environment where an agent represented by a green square starts from the starting point and can receive a reward by reaching the endpoint. However, there is a possibility that the agent may enter the red zone. The reward functions are set as follows: the agent receives a reward of  $-1$  after entering the red zone (left), and the agent receives a reward of  $0$  after entering the red zone (right). It is evident that in the left environment, the positional information of the red zone is useful to the agent, while in the right environment, the positional information of the red zone can be ignored by the agent. Thus, the agent should have different representations for the two environments.

Figure 3: The impacts of biases and reward functions on generalization

Although estimating different states with the same semantics during training is challenging, one effective approach to explicitly learn the underlying semantics is to introduce the adversarial method. For instance, [Rahman & Xue \(2023\)](#) aims to maximize expected return while minimizing the interference from adversarial examples generated by its own generator, StarGAN ([Choi et al., 2018](#)). This process ultimately facilitates robust policy learning and helps prevent the agent from overfitting irrelevant features in high-dimensional observations, inspiring us to incorporate an adversarial framework into our approach (Section 4.3).

However, StarGAN does not entirely eliminate the biases introduced by human prior knowledge. Specifically, the domain of the original input image is clustered using a Gaussian Mixture Model (GMM), which inherently introduces biases from the GMM. Furthermore, the number of clusters is often determined empirically, adding another layer of human influence.

Therefore, firstly, a sufficiently general agent should spontaneously learn robust representations for irrelevant features, rather than relying on biases introduced by human prior knowledge. Figure 3 (a) shows the potential impact of introducing biases into the model. Secondly, the entire pipeline for learning generalization must integrate the RL process, as the identification of irrelevant features is closely linked to the objectives of RL, particularly the configuration of the reward function. Figure 3 (b) demonstrates how different reward functions influence the agent's recognition of irrelevant information within a simple maze environment.

In summary, we conclude that a sufficiently general agent should possess two characteristics:

**(1) The agent is able to spontaneously learn robust representations for high-dimensional input without introducing any bias that benefits from human prior knowledge.**

**(2) The agent should adaptively adjust its representation of underlying semantics in response to changes in the reward function, demonstrating the ability to identify the semantics corresponding to specific objectives.**

Given these two points, we will introduce a dual-agent adversarial framework in the following section, which empowers agents with enhanced generalization capabilities.

#### 4.3 ADVERSARIAL POLICY LEARNING FRAMEWORK

In the previous analysis, we summarized the core challenges in the generalization of RL (Section 4.1) and the characteristics a general agent should possess (Section 4.2). However, generating adversarial

---

**Algorithm 2** Dual-agent adversarial policy learning
 

---

```

378
379
380 1: Initialize: Agent 1's encoder and policy  $\psi_1, \pi_1$ , agent 2's encoder and policy  $\psi_2, \pi_2$ 
381 2: Initialize: Reinforcement learning algorithm  $\mathcal{A}$ 
382 3: Initialize: Gradient descent optimizer  $\mathcal{O}$ 
383 4: while training do
384 5:   for  $i = 1, 2$  do
385 6:     Collect data  $\mathcal{D}_i$  using agent  $i$ 
386 7:     Calculate RL loss for agent  $i$ :  $\mathcal{L}_{\text{RL}} \leftarrow \mathcal{A}(\mathcal{D}_i)$ 
387 8:     Calculate KL loss for agent  $i$ :  $\mathcal{L}_{\text{KL}} \leftarrow D_{\text{KL}}^{\text{own}} - D_{\text{KL}}^{\text{other}}$  according to Equation (19)
388 9:     Calculate total loss for agent  $i$ :  $\mathcal{L} \leftarrow \mathcal{L}_{\text{RL}} + \alpha \mathcal{L}_{\text{KL}}$ 
389 10:    Update  $\psi_i, \pi_i, \psi_{3-i}, \pi_{3-i} \leftarrow \mathcal{O}(\mathcal{L}, \psi_i, \pi_i, \psi_{3-i})$ 
390 11:   end for
391 12: end while
392
393
394
  
```

---

samples through generative models introduces additional hyperparameters and training costs, and relies on carefully designed model architecture.

To address these issues, a viable solution is to attack the agent's encoder instead of directly generating adversarial samples. In this section, we introduce a dual-agent adversarial framework, which involves a game process between two homogeneous agents, as shown in Figure 4.

In particular, two symmetric agents are introduced in this framework, both agents have the capability to utilize their respective training data and update the other agent's encoder through back-propagation, which empowers them to perform adversarial attacks on each other. Since the two agents are equivalent in status, we take the perspective of agent 1 as an example. Agent 1 inputs its training data  $s_1$  into both its own encoder and the other agent's encoder, obtaining  $\psi_1(s_1)$  and  $\psi_2(s_1)$ , resulting in different representations of the same state  $s_1$ . The adversarial framework consists of two processes:

**Adversarial Attack on Opponent Agent.** To prevent the opponent agent from producing good actions, agent 1 attempts to alter the parameters of both encoders to influence agent 2's decision-making, where the KL divergence is used to quantify this distributional perturbation:

$$D_{\text{KL}}^{\text{other}} = D_{\text{KL}} [\pi_2(\cdot | \psi_2(s_1)), \pi_2(\cdot | \psi_1(s_1))]. \quad (17)$$

**Robust Defense Against Adversarial Threats.** Meanwhile, agent 1 itself attempts to remain robust to this influence, which can be expressed as

$$D_{\text{KL}}^{\text{own}} = D_{\text{KL}} [\pi_1(\cdot | \psi_1(s_1)), \pi_1(\cdot | \psi_2(s_1))]. \quad (18)$$

It should be noted that when agent 1 is performing adversarial attacks on agent 2's encoder  $\psi_2$ , the parameters of agent 2's policy network  $\pi_2$  are frozen during this stage, thus do not participate in gradient updates.

Overall, the goal of the agent is to maximize the perturbation  $D_{\text{KL}}^{\text{other}}$  while minimizing the self-inference  $D_{\text{KL}}^{\text{own}}$ , resulting in the loss function of the form:

$$\mathcal{L}_{\text{KL}} = D_{\text{KL}}^{\text{own}} - D_{\text{KL}}^{\text{other}}.$$

Since the adversarial process is coupled with the RL training process, the total loss is defined as

$$\mathcal{L} = \mathcal{L}_{\text{RL}} + \alpha \mathcal{L}_{\text{KL}}, \quad (20)$$

where  $\mathcal{L}_{\text{RL}}$  is the loss function using a specific RL algorithm,  $\alpha$  is the only additional hyperparameter. As the two agents are equivalent, the training processes for both agents are completely symmetrical. The pseudo-code of the adversarial policy learning process is shown in Algorithm 2.

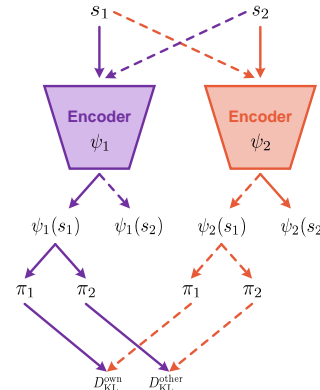


**Figure 4: Adversarial policy learning framework.**  $\psi_1$  and  $\pi_1$  represent the encoder and policy network of agent 1, while  $\psi_2$  and  $\pi_2$  represent the encoder and policy network of agent 2.  $s_1$  and  $s_2$  represent the training data for agent 1 and agent 2, respectively. Moreover, the solid lines indicate that the training data of each agent is input into its corresponding encoder, while dashed lines indicate that the training data of each agent is input into the other's encoder.

The overall loss comprises two components: the reinforcement learning loss term  $\mathcal{L}_{\text{RL}}$  and the adversarial loss term  $\mathcal{L}_{\text{KL}}$ . The adversarial loss facilitates a competitive interaction among agents and functions similarly to a form of regularization, effectively preventing agents from overfitting to irrelevant features in high-dimensional observations. With the alternate updating of the two agents, they will have to consider the truly useful underlying semantics, leading to better generalization performance, or mathematically speaking, a lower  $\mathbb{E}_{m, \tilde{m} \sim p_{\mathcal{M}_{\text{train}}}(\cdot)} \{D_{\text{KL}}[\pi_\theta(\cdot | s_m), \pi_\theta(\cdot | \bar{s}_m)]\}$  in constrained optimization problem (16).

In summary, our proposed adversarial policy learning framework is well in line with the two characteristics proposed in Section 4.2:

**(1) First, the framework does not introduce any additional biases, allowing the agents to learn the underlying semantics spontaneously.**

**(2) Second, the adversarial process and the reinforcement learning process are highly coupled, which means that the dependency between the reward signal and the corresponding representation can be modeled well.**

## 5 EXPERIMENTS

### 5.1 EXPERIMENTAL SETTINGS

**Benchmark.** Procgen (Cobbe et al., 2020) is an environment library specifically designed for reinforcement learning research, developed by OpenAI. It provides a diverse and procedurally generated set of platform games, allowing researchers to test the generalization capabilities of agents across different tasks and scenarios.

**Baselines.** We verify the performance of our proposed method compared with PPO (Schulman et al., 2017) and DAAC (Raileanu & Fergus, 2021) as the baselines for our comparative experiments.

**Training Settings.** In all experiments, we use the hyperparameters provided in the Appendix B unless otherwise specified. We referred to the original paper for hyperparameters specific to the algorithm. Following the recommendations of Cobbe et al. (2020), we run these methods on hard-level generalization tasks, training on eight environments of 500 levels and evaluating generalization performance on the full distribution of levels. We interact for 50M steps to consider running time. This is sufficient to assess the performance differences between our method and other baselines.

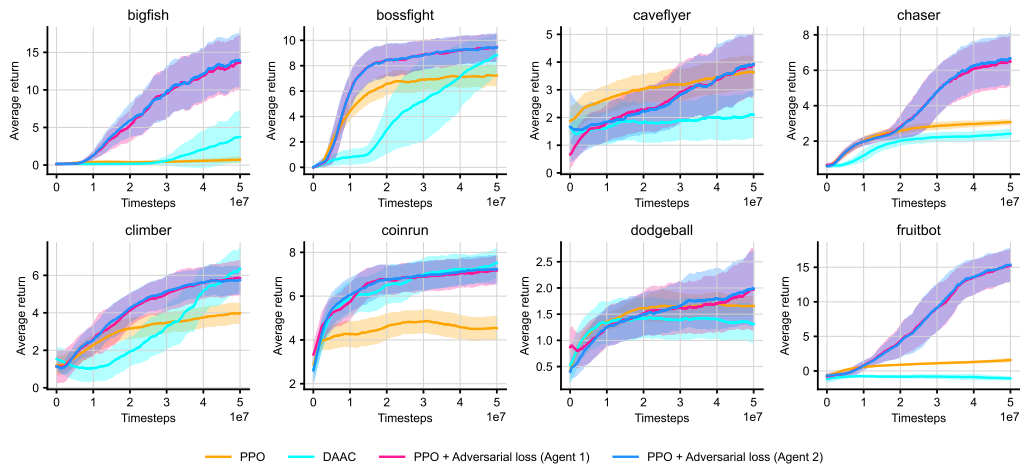


**Figure 5: Test performance curves of each method on eight hard-level Procgen games.** Each agent is trained on 500 training levels for 50M environment steps and evaluated on the full distribution of levels. The mean and standard deviation is shown across three random seeds.

486  
487  
488  
Table 1: **Average test performance** of PPO, DAAC and PPO with our adversarial loss on eight  
hard-level Progen games. The average return is shown across three random seeds.

Env. \ Method	PPO	DAAC	PPO + Adv. (Agent 1)	PPO + Adv. (Agent 2)
bigfish	0.485	1.193	7.904	<b>8.117</b>
bossfight	6.196	4.655	7.957	<b>7.970</b>
caveflyer	<b>3.162</b>	1.852	2.768	2.731
chaser	2.634	1.955	4.215	<b>4.270</b>
climber	3.233	3.299	4.473	<b>4.520</b>
coinrun	4.592	6.735	6.710	<b>6.803</b>
dodgeball	1.587	1.380	1.554	<b>1.593</b>
fruitbot	1.037	-0.860	8.027	<b>8.050</b>
<i>Average Score</i>	2.866	2.526	5.451	<b>5.507</b>

## 498 5.2 EXPERIMENT RESULTS

500 Our experimental results are illustrated in Figure 5 and Table 1. The data clearly demonstrate that  
501 directly integrating our adversarial framework with the Proximal Policy Optimization (PPO) algo-  
502 rithm leads to substantial performance enhancements across various environments. In particular,  
503 our PPO + Adv. methods consistently outperform the DAAC algorithm, which relies on carefully  
504 crafted model architectures and additional hyperparameters. For instance, in the chaser task, our  
505 agent achieves a score of 4.270, surpassing DAAC’s score of 1.955. This highlights not only the  
506 strength of our framework but also its potential to simplify model design while enhancing perfor-  
507 mance. In addition, the performance of our approach achieves an impressive score of 8.117 in  
508 bigfish, representing a remarkable increase of 1573% compared to the baseline PPO score of 0.485.  
509 Similarly, in the fruitbot environment, our method records a score of 8.050, a significant improve-  
510 ment of 676% over the PPO score of 1.037. These examples underscore the effectiveness of our  
511 adversarial approach in facilitating robust learning and adaptation in complex scenarios.

512 Overall, the average scores reveal that our methods yield an average score of 5.507, compared to  
513 2.866 for the standard PPO and 2.526 for DAAC. This improvement reflects a strong generaliza-  
514 tion capability, indicating that our framework enables agents to perform better across a range of  
515 environments, thereby enhancing their adaptability and resilience to variations in task conditions.

## 516 6 RELATED WORK

517 **Generalizable RL Methods.** Data augmentation methods are considered as effective solutions for  
518 enhancing the generalization of agents. Directly integrating existing data augmentation methods  
519 with RL algorithms can yield improvements (Laskin et al., 2020; Kostrikov et al., 2020; Zhang  
520 & Guo, 2021; Raileanu et al., 2021). Domain randomization techniques (Tobin et al., 2017; Yue  
521 et al., 2019; Slaoui et al., 2019; Lee et al., 2019; Mehta et al., 2020; Li et al., 2021) inject random  
522 disturbances representing variations in the simulated environment during the training process of RL,  
523 effectively enhancing the adaptability of RL agents to unknown environments.

524 **Adversarial Learning.** Adversarial learning has been proven to be a powerful learning framework  
525 (Goodfellow et al., 2014; Jiang et al., 2020; Dong et al., 2020). For instance, combining adversarial  
526 learning with randomization to enhance the generalization performance of agents (Pinto et al., 2017;  
527 Li et al., 2021; Rahman & Xue, 2023). In addition, adversarial attacks are also used to improve the  
528 robustness and generalization performance of agents (Gleave et al., 2019; Oikarinen et al., 2021).

## 531 7 CONCLUSION

532 This paper introduces a dual-agent adversarial framework designed to tackle the challenges of gen-  
533 eralization in reinforcement learning. By incorporating a competitive process between two agents,  
534 our framework leverages adversarial loss to enable both agents to spontaneously learn effective  
535 representations of high-dimensional observations, resulting in robust policies that effectively handle  
536 irrelevant features. Extensive experimental results demonstrate that this framework significantly en-  
537 hances both the training and generalization performance of baseline RL algorithms. Our findings  
538 indicate that the adversarial approach not only improves the resilience of RL agents but also repre-  
539 sents a meaningful advancement in the quest for generalizable reinforcement learning solutions.

540 REFERENCES  
541

- 542 Rishabh Agarwal, Marlos C Machado, Pablo Samuel Castro, and Marc G Bellemare. Contrastive  
543 behavioral similarity embeddings for generalization in reinforcement learning. *arXiv preprint*  
544 *arXiv:2101.05265*, 2021.
- 545 Ron Amit, Ron Meir, and Kamil Ciosek. Discount factor as a regularizer in reinforcement learning.  
546 In *International conference on machine learning*, pp. 269–278. PMLR, 2020.
- 547 Yunjey Choi, Minje Choi, Munyoung Kim, Jung-Woo Ha, Sunghun Kim, and Jaegul Choo. Star-  
548 gan: Unified generative adversarial networks for multi-domain image-to-image translation. In  
549 *Proceedings of the IEEE conference on computer vision and pattern recognition*, pp. 8789–8797,  
550 2018.
- 551 Karl Cobbe, Oleg Klimov, Chris Hesse, Taehoon Kim, and John Schulman. Quantifying generaliza-  
552 tion in reinforcement learning. In *International conference on machine learning*, pp. 1282–1289.  
553 PMLR, 2019.
- 554 Karl Cobbe, Chris Hesse, Jacob Hilton, and John Schulman. Leveraging procedural generation to  
555 benchmark reinforcement learning. In *International conference on machine learning*, pp. 2048–  
556 2056. PMLR, 2020.
- 557 Yinpeng Dong, Zhijie Deng, Tianyu Pang, Jun Zhu, and Hang Su. Adversarial distributional training  
558 for robust deep learning. *Advances in Neural Information Processing Systems*, 33:8270–8283,  
559 2020.
- 560 Dibya Ghosh, Jad Rahme, Aviral Kumar, Amy Zhang, Ryan P Adams, and Sergey Levine. Why  
561 generalization in rl is difficult: Epistemic pomdps and implicit partial observability. *Advances in*  
562 *neural information processing systems*, 34:25502–25515, 2021.
- 563 Adam Gleave, Michael Dennis, Cody Wild, Neel Kant, Sergey Levine, and Stuart Russell. Adver-  
564 sarial policies: Attacking deep reinforcement learning. *arXiv preprint arXiv:1905.10615*, 2019.
- 565 Ian Goodfellow, Jean Pouget-Abadie, Mehdi Mirza, Bing Xu, David Warde-Farley, Sherjil Ozair,  
566 Aaron Courville, and Yoshua Bengio. Generative adversarial nets. *Advances in neural information*  
567 *processing systems*, 27, 2014.
- 568 Ziyu Jiang, Tianlong Chen, Ting Chen, and Zhangyang Wang. Robust pre-training by adversarial  
569 contrastive learning. *Advances in neural information processing systems*, 33:16199–16210, 2020.
- 570 Sham Kakade and John Langford. Approximately optimal approximate reinforcement learning.  
571 In *Proceedings of the Nineteenth International Conference on Machine Learning*, pp. 267–274,  
572 2002.
- 573 Ezgi Korkmaz. A survey analyzing generalization in deep reinforcement learning. *arXiv preprint*  
574 *arXiv:2401.02349*, 2024.
- 575 Ilya Kostrikov, Denis Yarats, and Rob Fergus. Image augmentation is all you need: Regularizing  
576 deep reinforcement learning from pixels. *arXiv preprint arXiv:2004.13649*, 2020.
- 577 Misha Laskin, Kimin Lee, Adam Stooke, Lerrel Pinto, Pieter Abbeel, and Aravind Srinivas. Rein-  
578 forcement learning with augmented data. *Advances in neural information processing systems*, 33:  
579 19884–19895, 2020.
- 580 Kimin Lee, Kibok Lee, Jinwoo Shin, and Honglak Lee. Network randomization: A simple technique  
581 for generalization in deep reinforcement learning. *arXiv preprint arXiv:1910.05396*, 2019.
- 582 Bonnie Li, Vincent François-Lavet, Thang Doan, and Joelle Pineau. Domain adversarial reinforce-  
583 ment learning. *arXiv preprint arXiv:2102.07097*, 2021.
- 584 Zhuang Liu, Xuanlin Li, Bingyi Kang, and Trevor Darrell. Regularization matters in policy opti-  
585 mization. *arXiv preprint arXiv:1910.09191*, 2019.
- 586 Bhairav Mehta, Manfred Diaz, Florian Golemo, Christopher J Pal, and Liam Paull. Active domain  
587 randomization. In *Conference on Robot Learning*, pp. 1162–1176. PMLR, 2020.

- 594 Tuomas Oikarinen, Wang Zhang, Alexandre Megretski, Luca Daniel, and Tsui-Wei Weng. Robust  
 595 deep reinforcement learning through adversarial loss. *Advances in Neural Information Processing*  
 596 *Systems*, 34:26156–26167, 2021.
- 597 Lerrel Pinto, James Davidson, Rahul Sukthankar, and Abhinav Gupta. Robust adversarial reinforce-  
 598 ment learning. In *International conference on machine learning*, pp. 2817–2826. PMLR, 2017.
- 600 Md Masudur Rahman and Yexiang Xue. Adversarial style transfer for robust policy optimization in  
 601 deep reinforcement learning. *arXiv preprint arXiv:2308.15550*, 2023.
- 602 Roberta Raileanu and Rob Fergus. Decoupling value and policy for generalization in reinforcement  
 603 learning. In *International Conference on Machine Learning*, pp. 8787–8798. PMLR, 2021.
- 605 Roberta Raileanu, Maxwell Goldstein, Denis Yarats, Ilya Kostrikov, and Rob Fergus. Automatic  
 606 data augmentation for generalization in reinforcement learning. *Advances in Neural Information*  
 607 *Processing Systems*, 34:5402–5415, 2021.
- 608 John Schulman. Trust region policy optimization. *arXiv preprint arXiv:1502.05477*, 2015.
- 610 John Schulman, Philipp Moritz, Sergey Levine, Michael Jordan, and Pieter Abbeel. High-  
 611 dimensional continuous control using generalized advantage estimation. *arXiv preprint*  
 612 *arXiv:1506.02438*, 2015.
- 613 John Schulman, Filip Wolski, Prafulla Dhariwal, Alec Radford, and Oleg Klimov. Proximal policy  
 614 optimization algorithms. *arXiv preprint arXiv:1707.06347*, 2017.
- 616 Reda Bahi Slaoui, William R Clements, Jakob N Foerster, and Sébastien Toth. Robust visual domain  
 617 randomization for reinforcement learning. *arXiv preprint arXiv:1910.10537*, 2019.
- 618 Richard S Sutton. Reinforcement learning: An introduction. *A Bradford Book*, 2018.
- 620 Josh Tobin, Rachel Fong, Alex Ray, Jonas Schneider, Wojciech Zaremba, and Pieter Abbeel. Do-  
 621 main randomization for transferring deep neural networks from simulation to the real world. In  
 622 *2017 IEEE/RSJ international conference on intelligent robots and systems (IROS)*, pp. 23–30.  
 623 IEEE, 2017.
- 624 Xiangyu Yue, Yang Zhang, Sicheng Zhao, Alberto Sangiovanni-Vincentelli, Kurt Keutzer, and Bo-  
 625 qing Gong. Domain randomization and pyramid consistency: Simulation-to-real generalization  
 626 without accessing target domain data. In *Proceedings of the IEEE/CVF international conference*  
 627 *on computer vision*, pp. 2100–2110, 2019.
- 629 Hanping Zhang and Yuhong Guo. Generalization of reinforcement learning with policy-aware ad-  
 630 versarial data augmentation. *arXiv preprint arXiv:2106.15587*, 2021.
- 631 Huan Zhang, Hongge Chen, Chaowei Xiao, Bo Li, Mingyan Liu, Duane Boning, and Cho-Jui Hsieh.  
 632 Robust deep reinforcement learning against adversarial perturbations on state observations. *Ad-*  
 633 *vances in Neural Information Processing Systems*, 33:21024–21037, 2020.
- 635  
 636  
 637  
 638  
 639  
 640  
 641  
 642  
 643  
 644  
 645  
 646  
 647

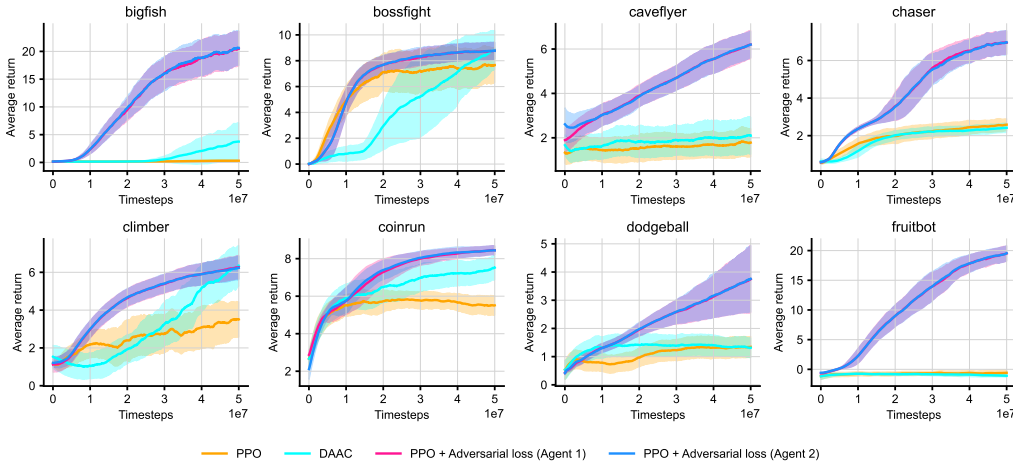
648  
649  
650  
651 A TRAINING RESULTS  
652  
653  
654  
655  
656  
657  
658  
659  
660  
661  
662  
663  
664  
665  
666  
667  
668  
669  
670  
671  
672

Figure 6: Train performance curves of each method on eight hard-level Procgen games.

## B HYPERPARAMETER SETTINGS

Table 2: Detailed hyperparameters in Procgen.

Hyperparameters	PPO (Schulman et al., 2017)	DAAC (Raileanu & Fergus, 2021)	PPO with adversarial loss (ours)
Environments per worker	64	64	64
Workers	4	4	4
Horizon	256	256	256
Learning rate	$5 \times 10^{-4}$	$5 \times 10^{-4}$	$5 \times 10^{-4}$
Learning rate decay	No	No	No
Optimizer	Adam	Adam	Adam
Total steps	50M	50M	50M
Batch size	16384	16384	16384
Update epochs	3	-	3
Mini-batches	8	8	8
Mini-batch size	2048	2048	2048
GAE parameter $\lambda$	0.95	0.95	0.95
Discount factor $\gamma$	0.999	0.999	0.999
Value loss coefficient $c_1$	0.5	-	0.5
Entropy loss coefficient $c_2$	0.01	0.01	0.01
Probability ratio parameter $\epsilon$	0.2	0.2	0.2
KL loss coefficient $\alpha$	-	-	1.0
Advantage loss coefficient $\alpha_a$	-	0.25	-
Policy update epochs $E_\pi$	-	1	-
Value update epochs $E_V$	-	9	-
Value updates after a policy update $N_\pi$	-	1	-

## C PROOFS

## C.1 PROOF OF ASSUMPTION 3.1

We now prove that  $p_{\mathcal{M}_{\text{train}}}(m)$  is a probability distribution, by integrating it, we obtain

$$\begin{aligned}
 \int_{\mathcal{M}_{\text{train}}} p_{\mathcal{M}_{\text{train}}}(m) dm &= \int_{\mathcal{M}_{\text{train}}} \frac{p_{\mathcal{M}}(m) \cdot \mathbb{I}(m \in \mathcal{M}_{\text{train}})}{M} dm \\
 &= \frac{1}{M} \int_{\mathcal{M}_{\text{train}}} p_{\mathcal{M}}(m) \cdot \mathbb{I}(m \in \mathcal{M}_{\text{train}}) dm \\
 &= \frac{1}{M} \int_{\mathcal{M}_{\text{train}}} p_{\mathcal{M}}(m) dm \\
 &= 1,
 \end{aligned} \tag{21}$$

concluding the proof.

702 C.2 PROOF OF THEOREM 3.2  
703704 We are trying to measure the difference between  $\zeta(\pi)$  and  $\eta(\pi)$ , which is  
705

$$\begin{aligned}
& |\zeta(\pi) - \eta(\pi)| \\
&= \left| \mathbb{E}_{m \sim p_{\mathcal{M}}(\cdot), \tau_m \sim \pi} \left[ \sum_{t=0}^{\infty} \gamma^t r_m(s_t^m, a_t^m) \right] - \mathbb{E}_{m \sim p_{\mathcal{M}_{\text{train}}}(\cdot), \tau_m \sim \pi} \left[ \sum_{t=0}^{\infty} \gamma^t r_m(s_t^m, a_t^m) \right] \right| \\
&= \left| \mathbb{E}_{m \sim p_{\mathcal{M}}(\cdot)} \left\{ \mathbb{E}_{\tau_m \sim \pi} \left[ \sum_{t=0}^{\infty} \gamma^t r_m(s_t^m, a_t^m) \right] \right\} - \mathbb{E}_{m \sim p_{\mathcal{M}_{\text{train}}}(\cdot)} \left\{ \mathbb{E}_{\tau_m \sim \pi} \left[ \sum_{t=0}^{\infty} \gamma^t r_m(s_t^m, a_t^m) \right] \right\} \right|. \tag{22}
\end{aligned}$$

714 First, we denote  $\mathbb{E}_{\tau_m \sim \pi} [\sum_{t=0}^{\infty} \gamma^t r_m(s_t^m, a_t^m)]$  as  $g_m(\pi)$ , then  
715

$$\begin{aligned}
|g_m(\pi)| &= \left| \mathbb{E}_{\tau_m \sim \pi} \left[ \sum_{t=0}^{\infty} \gamma^t r_m(s_t^m, a_t^m) \right] \right| \\
&= \left| \sum_{t=0}^{\infty} \sum_s \mathbb{P}(s_t^m = s | m, \pi) \sum_a \pi(a | s) \cdot \gamma^t r_m(s, a) \right| \\
&= \left| \sum_{t=0}^{\infty} \gamma^t \sum_s \mathbb{P}(s_t^m = s | m, \pi) \sum_a \pi(a | s) \cdot r_m(s, a) \right| \\
&\leq \sum_{t=0}^{\infty} \gamma^t \cdot \max_{m, s, a} |r_m(s, a)| \\
&= \frac{r_{\max}}{1 - \gamma}. \tag{23}
\end{aligned}$$

730 Second, according to Assumption 3.1, we have  
731

$$\begin{aligned}
& |\zeta(\pi) - \eta(\pi)| \\
&= \left| \mathbb{E}_{m \sim p_{\mathcal{M}}(\cdot)} [g_m(\pi)] - \mathbb{E}_{m \sim p_{\mathcal{M}_{\text{train}}}(\cdot)} [g_m(\pi)] \right| \\
&= \left| \int_{\mathcal{M}} p_{\mathcal{M}}(m) g_m(\pi) dm - \int_{\mathcal{M}_{\text{train}}} p_{\mathcal{M}_{\text{train}}}(m) g_m(\pi) dm \right| \\
&= \left| \int_{\mathcal{M}_{\text{train}}} p_{\mathcal{M}}(m) g_m(\pi) dm - \int_{\mathcal{M}_{\text{train}}} p_{\mathcal{M}_{\text{train}}}(m) g_m(\pi) dm + \int_{\mathcal{M} - \mathcal{M}_{\text{train}}} p_{\mathcal{M}}(m) g_m(\pi) dm \right| \\
&= \left| \left(1 - \frac{1}{M}\right) \int_{\mathcal{M}_{\text{train}}} p_{\mathcal{M}}(m) g_m(\pi) dm + \int_{\mathcal{M} - \mathcal{M}_{\text{train}}} p_{\mathcal{M}}(m) g_m(\pi) dm \right| \\
&\leq \left| \left(1 - \frac{1}{M}\right) \int_{\mathcal{M}_{\text{train}}} p_{\mathcal{M}}(m) g_m(\pi) dm \right| + \left| \int_{\mathcal{M} - \mathcal{M}_{\text{train}}} p_{\mathcal{M}}(m) g_m(\pi) dm \right| \\
&\leq \left( \frac{1}{M} - 1 \right) \cdot \frac{r_{\max}}{1 - \gamma} \cdot \int_{\mathcal{M}_{\text{train}}} p_{\mathcal{M}}(m) dm + \frac{r_{\max}}{1 - \gamma} \cdot \int_{\mathcal{M} - \mathcal{M}_{\text{train}}} p_{\mathcal{M}}(m) dm \\
&= \left( \frac{1}{M} - 1 \right) \cdot \frac{r_{\max}}{1 - \gamma} \cdot M + \frac{r_{\max}}{1 - \gamma} \cdot (1 - M) \\
&= \frac{2r_{\max}}{1 - \gamma} \cdot (1 - M). \tag{24}
\end{aligned}$$

752 Theorem 3.2 follows.  
753  
754  
755

### C.3 PROOF OF THEOREM 3.5

Let's start with Theorem 3.4 (Schulman, 2015), through a simple extension, by adding expectation  $\mathbb{E}_{m \sim p_{\mathcal{M}_{\text{train}}}(\cdot)}$  to the left and right sides of Theorem 3.4, we can derive the following lemma:

**Lemma C.1.** *Let  $m \sim p_{\mathcal{M}_{\text{train}}}(\cdot)$ , given any two policies,  $\pi$  and  $\tilde{\pi}$ , the following bound holds:*

$$\eta(\tilde{\pi}) \geq L_\pi(\tilde{\pi}) - \frac{4\gamma A_{\max}}{(1-\gamma)^2} \cdot \mathbb{E}_{m \sim p_{\mathcal{M}_{\text{train}}}(\cdot)} \left\{ D_{\text{TV}}^{\max} [\pi(\cdot | \phi_m(u)), \tilde{\pi}(\cdot | \phi_m(u))]^2 \right\}, \quad (25)$$

where  $A_{\max} = \max_{m,s,a} |A_m^\pi(s, a)|$  and

$$\begin{aligned} \eta(\tilde{\pi}) &= \eta(\pi) + \mathbb{E}_{m \sim p_{\mathcal{M}_{\text{train}}}(\cdot), s \sim \rho_{\tilde{\pi}}^m(\cdot), a \sim \tilde{\pi}(\cdot | s)} [A_m^\pi(s, a)], \\ L_\pi(\tilde{\pi}) &= \eta(\pi) + \mathbb{E}_{m \sim p_{\mathcal{M}_{\text{train}}}(\cdot), s \sim \rho_{\tilde{\pi}}^m(\cdot), a \sim \tilde{\pi}(\cdot | s)} [A_m^\pi(s, a)]. \end{aligned} \quad (26)$$

*Proof.* According to Theorem 3.4, given any  $m$ , we have

$$\begin{aligned} &\left| \mathbb{E}_{s \sim \rho_{\tilde{\pi}}^m(\cdot), a \sim \tilde{\pi}(\cdot | s)} [A_m^\pi(s, a)] - \mathbb{E}_{s \sim \rho_{\pi}^m(\cdot), a \sim \tilde{\pi}(\cdot | s)} [A_m^\pi(s, a)] \right| \\ &\leq \frac{4\gamma \max_{s,a} |A_m^\pi(s, a)|}{(1-\gamma)^2} \cdot D_{\text{TV}}^{\max} [\pi(\cdot | \phi_m(u)), \tilde{\pi}(\cdot | \phi_m(u))]^2, \end{aligned} \quad (27)$$

where the notation  $D_{\text{TV}}^{\max}(\cdot) = \max_u D_{\text{TV}}(\cdot)$ . Then

$$\begin{aligned} &|\eta(\tilde{\pi}) - L_\pi(\tilde{\pi})| \\ &= \left| \mathbb{E}_{m \sim p_{\mathcal{M}_{\text{train}}}(\cdot), s \sim \rho_{\tilde{\pi}}^m(\cdot), a \sim \tilde{\pi}(\cdot | s)} [A_m^\pi(s, a)] - \mathbb{E}_{m \sim p_{\mathcal{M}_{\text{train}}}(\cdot), s \sim \rho_{\pi}^m(\cdot), a \sim \tilde{\pi}(\cdot | s)} [A_m^\pi(s, a)] \right| \\ &= \left| \mathbb{E}_{m \sim p_{\mathcal{M}_{\text{train}}}(\cdot)} \left\{ \mathbb{E}_{s \sim \rho_{\tilde{\pi}}^m(\cdot), a \sim \tilde{\pi}(\cdot | s)} [A_m^\pi(s, a)] - \mathbb{E}_{s \sim \rho_{\pi}^m(\cdot), a \sim \tilde{\pi}(\cdot | s)} [A_m^\pi(s, a)] \right\} \right| \\ &\leq \mathbb{E}_{m \sim p_{\mathcal{M}_{\text{train}}}(\cdot)} \left\{ \left| \mathbb{E}_{s \sim \rho_{\tilde{\pi}}^m(\cdot), a \sim \tilde{\pi}(\cdot | s)} [A_m^\pi(s, a)] - \mathbb{E}_{s \sim \rho_{\pi}^m(\cdot), a \sim \tilde{\pi}(\cdot | s)} [A_m^\pi(s, a)] \right| \right\} \\ &\leq \mathbb{E}_{m \sim p_{\mathcal{M}_{\text{train}}}(\cdot)} \left\{ \frac{4\gamma \max_{s,a} |A_m^\pi(s, a)|}{(1-\gamma)^2} \cdot D_{\text{TV}}^{\max} [\pi(\cdot | \phi_m(u)), \tilde{\pi}(\cdot | \phi_m(u))]^2 \right\} \\ &\leq \frac{4\gamma A_{\max}}{(1-\gamma)^2} \cdot \mathbb{E}_{m \sim p_{\mathcal{M}_{\text{train}}}(\cdot)} \left\{ D_{\text{TV}}^{\max} [\pi(\cdot | \phi_m(u)), \tilde{\pi}(\cdot | \phi_m(u))]^2 \right\}, \end{aligned} \quad (28)$$

Lemma C.1 follows.  $\square$

Since the expectation of any constant is still this constant, i.e.,  $\mathbb{E}[c] = c$ , we have

$$\begin{aligned} &\mathbb{E}_{m \sim p_{\mathcal{M}_{\text{train}}}(\cdot)} \left\{ D_{\text{TV}}^{\max} [\pi(\cdot | \phi_m(u)), \tilde{\pi}(\cdot | \phi_m(u))]^2 \right\} \\ &= \mathbb{E}_{\tilde{m} \sim p_{\mathcal{M}_{\text{train}}}(\cdot)} \left\{ \mathbb{E}_{m \sim p_{\mathcal{M}_{\text{train}}}(\cdot)} \left\{ D_{\text{TV}}^{\max} [\pi(\cdot | \phi_m(u)), \tilde{\pi}(\cdot | \phi_m(u))]^2 \right\} \right\} \\ &= \mathbb{E}_{m, \tilde{m} \sim p_{\mathcal{M}_{\text{train}}}(\cdot)} \left\{ D_{\text{TV}}^{\max} [\pi(\cdot | \phi_m(u)), \tilde{\pi}(\cdot | \phi_m(u))]^2 \right\}, \end{aligned} \quad (29)$$

thus

$$\eta(\tilde{\pi}) \geq L_\pi(\tilde{\pi}) - \frac{4\gamma A_{\max}}{(1-\gamma)^2} \cdot \mathbb{E}_{m, \tilde{m} \sim p_{\mathcal{M}_{\text{train}}}(\cdot)} \left\{ D_{\text{TV}}^{\max} [\pi(\cdot | \phi_m(u)), \tilde{\pi}(\cdot | \phi_m(u))]^2 \right\}. \quad (30)$$

Now, denote  $u^* = \arg \max_u D_{\text{TV}} [\pi(\cdot | \phi_m(u)), \tilde{\pi}(\cdot | \phi_m(u))]^2$ , and based on the triangle inequality for total variation distance, we have

$$\begin{aligned} &\mathbb{E}_{m, \tilde{m} \sim p_{\mathcal{M}_{\text{train}}}(\cdot)} \left\{ D_{\text{TV}}^{\max} [\pi(\cdot | \phi_m(u)), \tilde{\pi}(\cdot | \phi_m(u))]^2 \right\} \\ &= \mathbb{E}_{m, \tilde{m} \sim p_{\mathcal{M}_{\text{train}}}(\cdot)} \left\{ D_{\text{TV}} [\pi(\cdot | \phi_m(u^*)), \tilde{\pi}(\cdot | \phi_m(u^*))]^2 \right\} \\ &\leq \mathbb{E}_{m, \tilde{m} \sim p_{\mathcal{M}_{\text{train}}}(\cdot)} \left\{ (D_{\text{TV}} [\pi(\cdot | \phi_m(u^*)), \pi(\cdot | \phi_{\tilde{m}}(u^*))] + D_{\text{TV}} [\pi(\cdot | \phi_{\tilde{m}}(u^*)), \tilde{\pi}(\cdot | \phi_{\tilde{m}}(u^*))] + \right. \\ &\quad \left. + D_{\text{TV}} [\tilde{\pi}(\cdot | \phi_m(u^*)), \tilde{\pi}(\cdot | \phi_{\tilde{m}}(u^*))]^2 \right\}, \end{aligned} \quad (31)$$

810 so that

$$\begin{aligned}
& \mathbb{E}_{m, \tilde{m} \sim p_{\mathcal{M}_{\text{train}}}(\cdot)} \left\{ D_{\text{TV}}^{\max} [\pi(\cdot | \phi_m(u)), \tilde{\pi}(\cdot | \phi_m(u))]^2 \right\} \\
& \leq \mathbb{E}_{m, \tilde{m} \sim p_{\mathcal{M}_{\text{train}}}(\cdot)} \left\{ D_{\text{TV}} [\pi(\cdot | \phi_m(u^*)), \pi(\cdot | \phi_{\tilde{m}}(u^*))]^2 \right\} \\
& + \mathbb{E}_{m, \tilde{m} \sim p_{\mathcal{M}_{\text{train}}}(\cdot)} \left\{ D_{\text{TV}} [\pi(\cdot | \phi_{\tilde{m}}(u^*)), \tilde{\pi}(\cdot | \phi_{\tilde{m}}(u^*))]^2 \right\} \\
& + \mathbb{E}_{m, \tilde{m} \sim p_{\mathcal{M}_{\text{train}}}(\cdot)} \left\{ D_{\text{TV}} [\tilde{\pi}(\cdot | \phi_m(u^*)), \tilde{\pi}(\cdot | \phi_{\tilde{m}}(u^*))]^2 \right\} \\
& + 2 \mathbb{E}_{m, \tilde{m} \sim p_{\mathcal{M}_{\text{train}}}(\cdot)} \left\{ D_{\text{TV}} [\pi(\cdot | \phi_m(u^*)), \pi(\cdot | \phi_{\tilde{m}}(u^*))] \cdot D_{\text{TV}} [\pi(\cdot | \phi_{\tilde{m}}(u^*)), \tilde{\pi}(\cdot | \phi_{\tilde{m}}(u^*))] \right\} \\
& + 2 \mathbb{E}_{m, \tilde{m} \sim p_{\mathcal{M}_{\text{train}}}(\cdot)} \left\{ D_{\text{TV}} [\pi(\cdot | \phi_m(u^*)), \pi(\cdot | \phi_{\tilde{m}}(u^*))] \cdot D_{\text{TV}} [\tilde{\pi}(\cdot | \phi_m(u^*)), \tilde{\pi}(\cdot | \phi_{\tilde{m}}(u^*))] \right\} \\
& + 2 \mathbb{E}_{m, \tilde{m} \sim p_{\mathcal{M}_{\text{train}}}(\cdot)} \left\{ D_{\text{TV}} [\pi(\cdot | \phi_{\tilde{m}}(u^*)), \tilde{\pi}(\cdot | \phi_{\tilde{m}}(u^*))] \cdot D_{\text{TV}} [\tilde{\pi}(\cdot | \phi_m(u^*)), \tilde{\pi}(\cdot | \phi_{\tilde{m}}(u^*))] \right\}. \tag{32}
\end{aligned}$$

825 Next, according to the Cauchy-Schwarz inequality, i.e.,  $X$  and  $Y$  are two positive random variables,  
826 then  $\mathbb{E}[XY] \leq \sqrt{\mathbb{E}[X^2] \cdot \mathbb{E}[Y^2]}$ , we obtain

$$\begin{aligned}
& \mathbb{E}_{m, \tilde{m} \sim p_{\mathcal{M}_{\text{train}}}(\cdot)} \left\{ D_{\text{TV}}^{\max} [\pi(\cdot | \phi_m(u)), \tilde{\pi}(\cdot | \phi_m(u))]^2 \right\} \\
& \leq \mathbb{E}_{m, \tilde{m} \sim p_{\mathcal{M}_{\text{train}}}(\cdot)} \left\{ D_{\text{TV}} [\pi(\cdot | \phi_m(u^*)), \pi(\cdot | \phi_{\tilde{m}}(u^*))]^2 \right\} \\
& + \mathbb{E}_{m, \tilde{m} \sim p_{\mathcal{M}_{\text{train}}}(\cdot)} \left\{ D_{\text{TV}} [\pi(\cdot | \phi_{\tilde{m}}(u^*)), \tilde{\pi}(\cdot | \phi_{\tilde{m}}(u^*))]^2 \right\} \\
& + \mathbb{E}_{m, \tilde{m} \sim p_{\mathcal{M}_{\text{train}}}(\cdot)} \left\{ D_{\text{TV}} [\tilde{\pi}(\cdot | \phi_m(u^*)), \tilde{\pi}(\cdot | \phi_{\tilde{m}}(u^*))]^2 \right\} \\
& + 2 \sqrt{\mathbb{E}_{m, \tilde{m} \sim p_{\mathcal{M}_{\text{train}}}(\cdot)} \left\{ D_{\text{TV}} [\pi(\cdot | \phi_m(u^*)), \pi(\cdot | \phi_{\tilde{m}}(u^*))]^2 \right\} \cdot \mathbb{E}_{m, \tilde{m} \sim p_{\mathcal{M}_{\text{train}}}(\cdot)} \left\{ D_{\text{TV}} [\pi(\cdot | \phi_{\tilde{m}}(u^*)), \tilde{\pi}(\cdot | \phi_{\tilde{m}}(u^*))]^2 \right\}} \\
& + 2 \sqrt{\mathbb{E}_{m, \tilde{m} \sim p_{\mathcal{M}_{\text{train}}}(\cdot)} \left\{ D_{\text{TV}} [\pi(\cdot | \phi_m(u^*)), \pi(\cdot | \phi_{\tilde{m}}(u^*))]^2 \right\} \cdot \mathbb{E}_{m, \tilde{m} \sim p_{\mathcal{M}_{\text{train}}}(\cdot)} \left\{ D_{\text{TV}} [\tilde{\pi}(\cdot | \phi_m(u^*)), \tilde{\pi}(\cdot | \phi_{\tilde{m}}(u^*))]^2 \right\}} \\
& + 2 \sqrt{\mathbb{E}_{m, \tilde{m} \sim p_{\mathcal{M}_{\text{train}}}(\cdot)} \left\{ D_{\text{TV}} [\pi(\cdot | \phi_{\tilde{m}}(u^*)), \tilde{\pi}(\cdot | \phi_{\tilde{m}}(u^*))]^2 \right\} \cdot \mathbb{E}_{m, \tilde{m} \sim p_{\mathcal{M}_{\text{train}}}(\cdot)} \left\{ D_{\text{TV}} [\tilde{\pi}(\cdot | \phi_m(u^*)), \tilde{\pi}(\cdot | \phi_{\tilde{m}}(u^*))]^2 \right\}} \\
& \leq \mathfrak{D}_2 + \mathfrak{D}_1 + \mathfrak{D}_3 + 2\sqrt{\mathfrak{D}_2\mathfrak{D}_1} + 2\sqrt{\mathfrak{D}_2\mathfrak{D}_3} + 2\sqrt{\mathfrak{D}_1\mathfrak{D}_3} \\
& = \left( \sqrt{\mathfrak{D}_1} + \sqrt{\mathfrak{D}_2} + \sqrt{\mathfrak{D}_3} \right)^2. \tag{33}
\end{aligned}$$

848 Finally, by combining the inequality (30) and inequality (33), we derive

$$\eta(\tilde{\pi}) \geq L_{\pi}(\tilde{\pi}) - \frac{4\gamma A_{\max}}{(1-\gamma)^2} \cdot \left( \sqrt{\mathfrak{D}_1} + \sqrt{\mathfrak{D}_2} + \sqrt{\mathfrak{D}_3} \right)^2, \tag{34}$$

852 concluding the proof of Theorem 3.5.

853  
854  
855  
856  
857  
858  
859  
860  
861  
862  
863